nature immunology

The transcription factors Blimp-1 and IRF4 jointly control the differentiation and function of effector regulatory T cells

Erika Cretney[1,2,6], Annie Xin[1,2,6], Wei Shi[1,3], Martina Minnich[4], Frederick Masson[1,2], Maria Miasari[1,2], Gabrielle T Belz[1,2], Gordon K Smyth[1,5], Meinrad Busslinger[4], Stephen L Nutt[1,2] & Axel Kallies[1,2]

Regulatory T cells (T_{reg} cells) are required for peripheral tolerance. Evidence indicates that T_{reg} cells can adopt specialized differentiation programs in the periphery that are controlled by transcription factors usually associated with helper T cell differentiation. Here we demonstrate that expression of the transcription factor Blimp-1 defined a population of T_{reg} cells that localized mainly to mucosal sites and produced IL-10. Blimp-1 was required for IL-10 production by these cells and for their tissue homeostasis. We provide evidence that the transcription factor IRF4, but not the transcription factor T-bet, was essential for Blimp-1 expression and for the differentiation of all effector T_{reg} cells. Thus, our study defines a differentiation pathway that leads to the acquisition of T_{reg} cell effector functions and requires both IRF4 and Blimp-1.

Naturally occurring $CD4^+Foxp3^+$ regulatory T cells (T_{reg} cells) are derived from the thymus and are essential for the preservation of immune homeostasis and suppression of autoimmune pathology[1,2]. T_{reg} cells depend on interleukin 2 (IL-2) for their maintenance and peripheral homeostasis and consequently have high expression of CD25 (the IL-2 receptor α-chain)[3,4]. Many aspects of the differentiation and function of T_{reg} cells are controlled by the forkhead family transcription factor Foxp3 (ref. 5). Foxp3 deficiency results in an absence of T_{reg} cells and severe systemic autoimmune pathology in mice and humans[6,7]. T_{reg} cells exert their immunoregulatory functions through a variety of effector mechanisms, such as upregulation of the immune modulator CTLA-4 (refs. 8,9), consumption of IL-2 (ref. 10) and the production of immunomodulatory cytokines such as IL-10 (ref. 1). Although IL-10 production by T_{reg} cells is not required for the suppression of systemic autoimmunity, it is essential for the control of local immune responses in the lungs and intestinal tract[11].

Analysis of human $Foxp3^+$ T cells has provided evidence for the existence of a subset of T_{reg} cells with high expression of IL-10 and the inducible costimulator ICOS[12]. Similarly, subpopulations of mouse T_{reg} cells with an activated phenotype and distinct homing characteristics are enriched in IL-10 (refs. 13–15). In line with those reports, studies of IL-10 reporter mice have demonstrated that $Foxp3^+IL\text{-}10^-$ cells predominate in lymphoid tissues, whereas $Foxp3^+IL\text{-}10^+$ cells tend to localize to the intestinal tract[16].

It has become apparent that the phenotypic and functional diversity of T_{reg} cells is driven by specific transcription factors distinct from Foxp3. The transcription factor IRF4 acts downstream of Foxp3, which suggests that T_{reg} cells use the transcriptional machinery of T helper type 2 (T_H2) effector cells to specifically control this subset of helper T cells[17]. In an analogous manner, the transcription factors T-bet and STAT3 control the homeostasis and function of T_{reg} cells during T_H1 and T_H17 inflammation, respectively[18,19]. Notably, IL-10 acts as an effector molecule of all these specialized T_{reg} cell subsets[17–19].

The transcription factor Blimp-1 is encoded by *Prdm1* (called '*Blimp1*' here), which is a target of Foxp3 in T_{reg} cells[20,21]. Blimp-1 is a transcriptional repressor well known for its role in promoting the differentiation of plasma cells[22–24]. It is also required for the maintenance of T cell homeostasis, as mice that lack Blimp-1 specifically in T cells, or mice reconstituted with Blimp-1-deficient fetal liver cells, accumulate activated T cells and develop immune pathology, including colitis and lung inflammation[25,26]. In T cells, Blimp-1 is induced by IL-2 but then represses *Il2* transcription in a negative feedback loop[27,28]. In $CD4^+$ T cells, Blimp-1 attenuates T_H1 differentiation[29] and represses the formation of follicular helper T cells[30]. In mouse models of virus infection, Blimp-1 is required for the differentiation of $CD8^+$ cytotoxic effector T cells and functional memory cells[31,32].

Although the severe T cell–mediated immune pathology observed in Blimp-1-deficient mice[25,26] suggests that Blimp-1 has a critical role in T_{reg} cell function, studies so far have not been conclusive[25,26]. Here we show that *Blimp1* expression was restricted to a subpopulation of mature effector T_{reg} cells, where it was required for IL-10 production and high ICOS expression. Blimp-1 limited expression of

[1]The Walter and Eliza Hall Institute of Medical Research, Parkville, Victoria, Australia. [2]Department of Medical Biology, The University of Melbourne, Parkville, Victoria, Australia. [3]Department of Computer Science and Software Engineering, The University of Melbourne, Parkville, Victoria, Australia. [4]Research Institute of Molecular Pathology, Vienna Biocenter, Vienna, Austria. [5]Department of Mathematics and Statistics, The University of Melbourne, Parkville, Victoria, Australia. [6]These authors contributed equally to this study. Correspondence should be addressed to A.K. (kallies@wehi.edu.au) or S.L.N. (nutt@wehi.edu.au).

Received 11 November 2009; accepted 4 February 2011; published online 6 March 2011; doi:10.1038/ni.2006

the prosurvival molecule Bcl-2 and the chemokine receptor CCR6, thereby leading to the accumulation of effector T_{reg} cells in mucosal sites in the absence of Blimp-1. We further found that IRF4 directly regulated *Blimp1* expression in T_{reg} cells and was indispensable for the generation of all effector T_{reg} cells. Blimp-1 and IRF4 acted together to directly regulate the expression of IL-10 and CCR6. Thus, our study demonstrates a central role for the IRF4–Blimp-1 axis in the function and homeostasis of T_{reg} cells.

RESULTS

Expression of Blimp-1 in IL-10-producing T_{reg} cells

T_{reg} cells are enriched in *Blimp1* mRNA[25,26]. To examine the expression of *Blimp1* in T_{reg} cells, we made use of the reporter function of a *Blimp1*^{GFP} allele, which allows monitoring of *Blimp1* expression at the single-cell level via expression of green fluorescent protein (GFP) as a surrogate marker[33]. Flow cytometry of splenocytes from naive *Blimp1*$^{+/GFP}$ mice showed that 8–12% of the CD4$^+$CD25$^+$ T cells expressed GFP (**Fig. 1a**). The proportion of Blimp1–GFP$^+$ cells was over 20% greater in aged mice (**Supplementary Fig. 1a**). Real-time PCR confirmed that GFP expression precisely correlated with expression of *Blimp1* mRNA (**Fig. 1b**). The percentage of Blimp-1–GFP$^+$ T_{reg} cells in mesenteric lymph nodes of *Blimp1*$^{+/GFP}$ mice was similar to that in the spleen, but it was lower in the thymus (2–4%) and peripheral lymph nodes (5–8%; **Fig. 1c** and data not shown). Both Blimp-1–GFP$^+$ and Blimp-1–GFP$^-$ CD25$^+$CD4$^+$ T cells expressed Foxp3 protein and mRNA (**Fig. 1d** and **Supplementary Fig. 1b**) and thus were true T_{reg} cells. In support of that conclusion, sorted Blimp-1–GFP$^+$ and Blimp-1–GFP$^-$ T_{reg} cells efficiently suppressed the proliferation of CD4$^+$CD25$^-$ T cells *in vitro* (**Fig. 1e**).

Flow cytometry of T_{reg} cells showed high expression of the integrin CD103, the leukocyte marker CD44, ICOS, the immunomodulatory receptor GITR, the costimulatory molecule CD38 and the activation marker CD69 on Blimp-1–GFP$^+$ cells, whereas expression of the lymph node–homing receptor CD62L was low, consistent with an effector phenotype (**Fig. 2a**). As the phenotype of Blimp-1–GFP$^+$ T_{reg} cells resembled that of IL-10-producing T_{reg} cells in humans[12] and mice[13,16], we sorted these cells according to their expression of Blimp-1–GFP and examined IL-10 expression by quantitative RT-PCR and cytokine bead array. IL-10 was restricted to Blimp-1-expressing cells. The amount of IL-10 in these cells was significantly higher than that in conventional CD25$^-$CD62L$^-$ effector-memory or CD25$^-$CD62L$^+$ naive CD4$^+$ T cells (**Fig. 2b**). Expression of the gene encoding transforming growth factor-β was similar in both T_{reg} cell populations (**Supplementary Fig. 1c**). As expected, production of IFN-γ, a T_H1 effector cytokine, was restricted to conventional effector-memory CD4$^+$ T cells and was almost undetectable in T_{reg} cells (**Fig. 2b**). Consistent with the specific requirement for IL-10 in the control of mucosal immune responses[11,16], analysis of Peyer's patches, intraepithelial lymphocytes and bronchoalveolar fluid of the lung showed they had a very large proportion of Blimp-1–GFP$^+$ T_{reg} cells (**Fig. 2c** and data not shown). Blimp-1–GFP$^+$ T_{reg} cells had high expression of two other transcription factors, IRF4 and T-bet (encoded by *Tbx21*), both of which have been linked to T_{reg} cell differentiation and IL-10 production[17,18] (**Fig. 2d**). These data demonstrate that Blimp-1 is expressed in a subset of Foxp3$^+$ T_{reg} cells with an effector phenotype that produce IL-10.

IL-10 production in T_{reg} cells requires Blimp-1

Blimp-1-deficient mice develop severe T cell–mediated immune pathology despite the presence of Foxp3$^+$ T cells[25]. Reconstitution of mice with a mixture of wild-type and Blimp-1-deficient bone marrow substantially delays pathology[25], which suggests that wild-type T_{reg} cells can suppress the pathological activation of Blimp-1-deficient T cells. To determine whether Blimp-1 has an intrinsic role in T_{reg} cells, we generated mixed chimeric mice containing Ly5.2$^+$*Blimp1*$^{GFP/GFP}$ and Ly5.1$^+$ wild-type bone marrow, which allowed direct comparison of Blimp-1-sufficient and Blimp-1-deficient T_{reg} cells. Both wild-type and Blimp-1-deficient cells contributed to the splenic T_{reg} cell compartment in these mice (**Fig. 3a**). In the *Blimp1*$^{GFP/GFP}$ T cell compartment, large numbers of Blimp-1–GFP$^+$ CD25$^+$CD4$^+$ T cells were present that expressed Foxp3 and had a phenotype similar to that of their counterparts in *Blimp1*$^{+/GFP}$ mice (**Fig. 3a**,**b** and **Supplementary Fig. 2a**,**b**), which indicated that Blimp-1 was not required for the generation of effector T_{reg} cells. In line with that conclusion, wild-type and Blimp-1-deficient T_{reg} cells expressed similar amounts of CTLA-4, and both populations generated ICOS$^+$CD103$^+$ cells (**Supplementary Fig. 2c**).

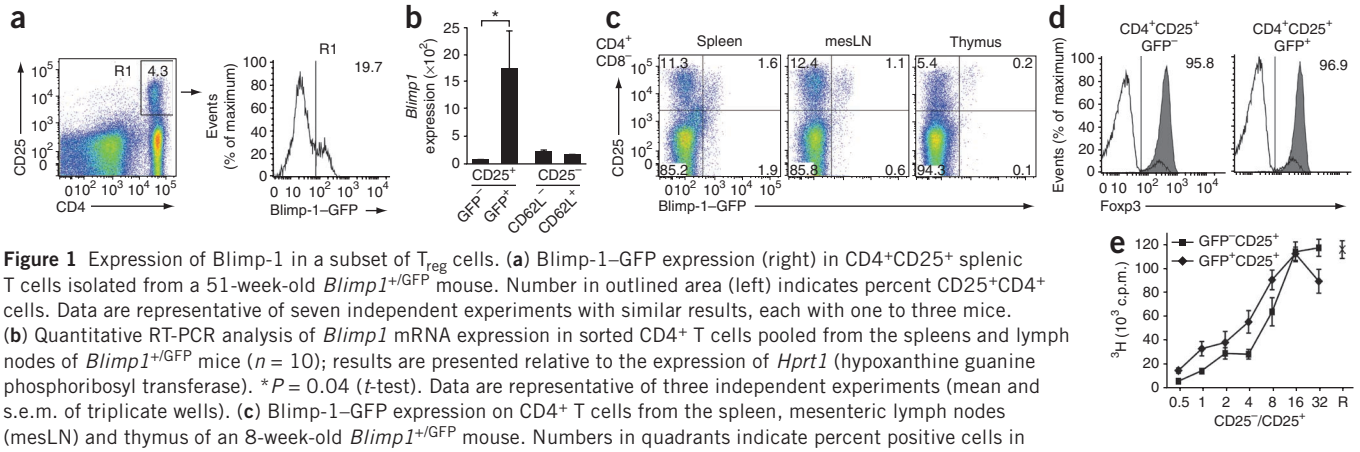

Figure 1 Expression of Blimp-1 in a subset of T_{reg} cells. (**a**) Blimp-1–GFP expression (right) in CD4$^+$CD25$^+$ splenic T cells isolated from a 51-week-old *Blimp1*$^{+/GFP}$ mouse. Number in outlined area (left) indicates percent CD25$^+$CD4$^+$ cells. Data are representative of seven independent experiments with similar results, each with one to three mice. (**b**) Quantitative RT-PCR analysis of *Blimp1* mRNA expression in sorted CD4$^+$ T cells pooled from the spleens and lymph nodes of *Blimp1*$^{+/GFP}$ mice ($n = 10$); results are presented relative to the expression of *Hprt1* (hypoxanthine guanine phosphoribosyl transferase). *$P = 0.04$ (*t*-test). Data are representative of three independent experiments (mean and s.e.m. of triplicate wells). (**c**) Blimp-1–GFP expression on CD4$^+$ T cells from the spleen, mesenteric lymph nodes (mesLN) and thymus of an 8-week-old *Blimp1*$^{+/GFP}$ mouse. Numbers in quadrants indicate percent positive cells in each. Data are representative of three to eight experiments. (**d**) Foxp3 expression in splenic CD4$^+$CD25$^+$ T cells (filled histograms) and CD4$^+$CD25$^-$ T cells (open histograms) pooled from *Blimp1*$^{+/GFP}$ mice ($n = 3$) and isolated according to Blimp-1–GFP expression. Numbers in plots indicate percent Foxp3$^+$ cells. Data are representative of two independent experiments. (**e**) Proliferation (assessed as [^{3}H]thymidine incorporation) of CD4$^+$CD25$^-$ responder T cells (CD25$^-$) cultured *in vitro* at various ratios (horizontal axis) with GFP$^-$ or GFP$^+$ CD4$^+$CD25$^+$ T cells (CD25$^+$) pooled from the spleens and lymph nodes of *Blimp1*$^{+/GFP}$ mice. R (far right), responder cells cultured without CD4$^+$CD25$^+$ cells. Data are representative of two independent experiments with similar results (mean ± s.e.m. of triplicate wells).

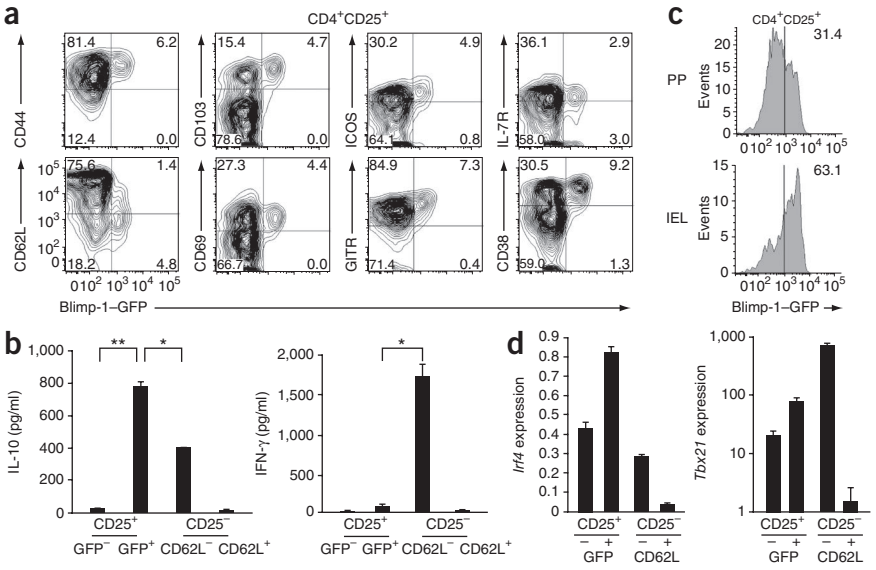

Figure 2 Blimp-1-expressing T_{reg} cells have an effector phenotype, produce IL-10 and localize to mucosal sites. (**a**) Flow cytometry of $CD4^+CD25^+$ T cells from the mesenteric lymph nodes of *Blimp1*$^{+/GFP}$ mice. Numbers in quadrants indicate percent cells in each. (**b**) Cytokine production by pooled *Blimp1*$^{+/GFP}$ splenic and lymph node $CD4^+$ T cells sorted according to various markers (horizontal axis) and stimulated for 24 h with monoclonal anti-CD3 and anti-CD28. $*P = 0.005$ and $**P = 0.0005$ (*t*-test). (**c**) Blimp-1–GFP expression in $CD4^+CD25^+$ T cells from Peyer's patches (PP) and among intraepithelial lymphocytes (IEL) of *Blimp1*$^{+/GFP}$ mice. Numbers in plots indicate percent Blimp-1–GFP^+ cells. (**d**) Quantitative RT-PCR analysis of the expression of *Irf4* and *Tbx21* in *Blimp1*$^{+/GFP}$ T_{reg} cells and conventional $CD4^+$ T cell populations sorted as in **b**; results are presented relative to *Hprt1* expression. Data are representative of two to three experiments with two to three mice each (**a**,**c**) or three independent experiments (**b**,**d**; mean and s.d. (**b**) or s.e.m. (**d**)).

T_{reg} cells isolated from mice that lack Blimp-1 in the T cell compartment do not contain *Il10* transcripts[25,26]. Although that is consistent with an essential role for Blimp-1 in the expression of IL-10 by T_{reg} cells, it could also be a consequence of the perturbed cytokine environment due to ongoing inflammation and immune pathology in Blimp-1-deficient mice. Blimp-1-deficient T_{reg} cells isolated from healthy mixed chimeric mice as described above failed to secrete IL-10, and *Il10* transcripts were almost completely undetectable regardless of GFP expression (**Fig. 3c** and **Supplementary Fig. 3a**). These data indicate that Blimp-1 is dispensable for the formation of effector T_{reg} cells but is essential for their ability to produce IL-10.

Blimp-1 regulates T_{reg} cell homeostasis and activation

Quantitative analysis of lymph node $CD4^+$ T cells of chimeric mice generated with a mixture of wild-type and *Blimp1*$^{GFP/GFP}$ bone marrow showed there were similar proportions of $Foxp3^+$ T_{reg} cells in the *Blimp1*$^{GFP/GFP}$ and wild-type compartments (**Fig. 3d**,**e**), which indicated that Blimp-1 does not have a role in the homeostasis of naive T_{reg} cells. In contrast, Blimp-1-deficient T_{reg} cells were more abundant than wild-type cells in the spleen and Peyer's patches and were considerably overrepresented among lymphocytes of the gastrointestinal epithelium and bronchoalveolar fluid of the lungs (**Fig. 3d**,**e** and **Supplementary Fig. 3b**), which suggested that Blimp-1 controls the tissue homeostasis of effector T_{reg} cells.

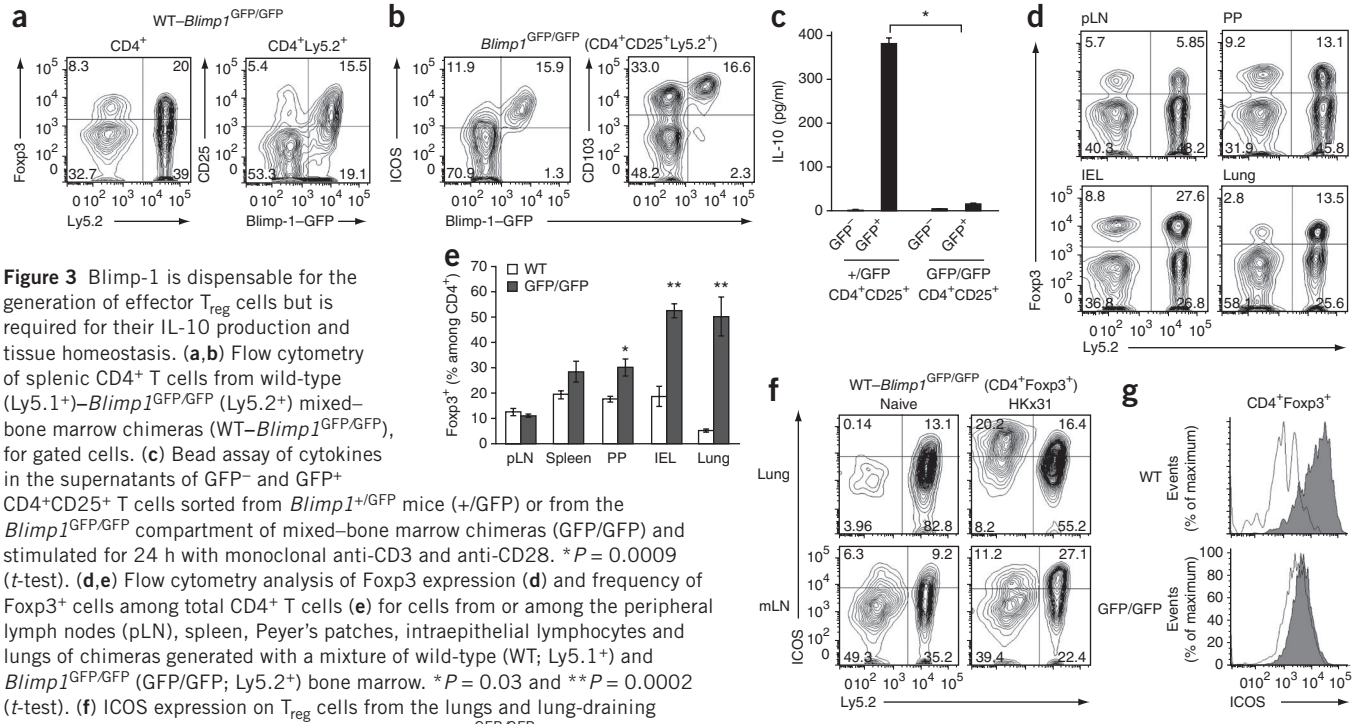

Figure 3 Blimp-1 is dispensable for the generation of effector T_{reg} cells but is required for their IL-10 production and tissue homeostasis. (**a**,**b**) Flow cytometry of splenic $CD4^+$ T cells from wild-type ($Ly5.1^+$)–*Blimp1*$^{GFP/GFP}$ ($Ly5.2^+$) mixed–bone marrow chimeras (WT–*Blimp1*$^{GFP/GFP}$), for gated cells. (**c**) Bead assay of cytokines in the supernatants of GFP^- and GFP^+ $CD4^+CD25^+$ T cells sorted from *Blimp1*$^{+/GFP}$ mice (+/GFP) or from the *Blimp1*$^{GFP/GFP}$ compartment of mixed–bone marrow chimeras (GFP/GFP) and stimulated for 24 h with monoclonal anti-CD3 and anti-CD28. $*P = 0.0009$ (*t*-test). (**d**,**e**) Flow cytometry analysis of Foxp3 expression (**d**) and frequency of $Foxp3^+$ cells among total $CD4^+$ T cells (**e**) for cells from or among the peripheral lymph nodes (pLN), spleen, Peyer's patches, intraepithelial lymphocytes and lungs of chimeras generated with a mixture of wild-type (WT; $Ly5.1^+$) and *Blimp1*$^{GFP/GFP}$ (GFP/GFP; $Ly5.2^+$) bone marrow. $*P = 0.03$ and $**P = 0.0002$ (*t*-test). (**f**) ICOS expression on T_{reg} cells from the lungs and lung-draining mediastinal lymph nodes (mLN) of wild-type–*Blimp1*$^{GFP/GFP}$ mixed chimeras before (Naive) 10 d after (HKx31) infection with influenza virus (strain HKx31). (**g**) ICOS expression on wild-type and *Blimp1*$^{GFP/GFP}$ $Foxp3^+CD4^+$ cells in the lungs of naive mice (open histograms) and influenza-infected mice (filled histograms). Numbers in quadrants (**a**,**b**,**d**,**f**) indicate percent cells in each. Data are representative of two to three independent experiments with similar results, each with three to five mice per group (mean and s.e.m. of triplicate wells in **c**; mean and s.d. in **e**).

To assess the role of Blimp-1 in the activation and tissue migration of T_{reg} cells during inflammation, we examined ICOS expression and the recruitment of T_{reg} cells into the lungs and the lung-draining mediastinal lymph nodes of naive and influenza virus–infected mixed–bone marrow chimeras at the peak of the antiviral T cell response. After infection, both wild-type and Blimp-1-deficient T_{reg} cells were efficiently recruited into the lungs, but only wild-type T_{reg} cells upregulated ICOS expression, whereas Blimp-1-deficient T_{reg} cells failed to substantially increase their expression of ICOS (**Fig. 3f**,**g**). This suggests that Blimp-1 deletion impairs effector T_{reg} cell activation.

Inducible *Blimp1* expression in T_{reg} cells

To assess the properties of Blimp-1-expressing T_{reg} cells *in vivo*, we made use of a T cell–induced colitis model of immunosuppression[34]. We injected mice deficient in recombination-activating gene 1 (*Rag1*$^{-/-}$ mice) with colitogenic CD4$^+$CD25$^-$ T cells and with purified congenically marked populations of Blimp-1–GFP$^-$ or Blimp-1–GFP$^+$ T_{reg} cells isolated from *Blimp1*$^{+/GFP}$ mice. We monitored the recipient mice for weight loss and analyzed them after 8 weeks. Both populations were able to suppress colitis induced by CD4$^+$CD25$^-$ T cells (data not shown). Analysis of the transferred T_{reg} cells showed that most of the initially Blimp-1–GFP$^-$ T_{reg} cells had induced Blimp-1–GFP expression in the course of the experiment, whereas Blimp-1–GFP$^+$ T_{reg} cells retained their phenotype (**Fig. 4a**). Furthermore, Blimp-1–GFP$^-$ T_{reg} cells had produced more T_{reg} cells than their GFP$^+$ counterparts had produced at the completion of the experiment (**Fig. 4b**). These data indicate that Blimp-1$^-$ T_{reg} cells can mature into Blimp-1$^+$ effector T_{reg} cells in the periphery and support our conclusion that Blimp-1 controls T_{reg} cell homeostasis.

As IL-2 has a key role in the survival and function of T_{reg} cells[3,4] and can induce *Blimp1* expression in conventional CD4$^+$ T cells[27,28], we investigated whether increasing the IL-2 concentration by injecting complexes of IL-2 and antibody to IL-2 (anti-IL-2)[35] would modulate *Blimp1* expression in T_{reg} cells *in vivo*. We observed seven- to tenfold more T_{reg} cells after administration of IL-2–anti-IL-2 complexes. Although both Blimp-1–GFP$^-$ and Blimp-1–GFP$^+$ T_{reg} cells were greater in absolute number, the proportion of Blimp-1–GFP$^+$ T_{reg} cells was much greater after induction by IL-2–anti-IL-2 complexes (**Fig. 4c** and **Supplementary Fig. 4a**). A similar increase in the fraction of Blimp-1-expressing T_{reg} cells occurred after repeated injection of *Blimp1*$^{+/GFP}$ mice with antibody to the costimulatory molecule CD40 (**Fig. 4d**). This protocol induces considerable T_H1-type inflammation[18], which suggests that inflammatory signals contribute to Blimp-1 induction in T_{reg} cells. Consistent with that conclusion, purified T_{reg} cells cultured in the presence of IL-2 had moderate expression of Blimp-1–GFP, whereas culture of T_{reg} cells with IL-2 in combination with inflammatory cytokines such as IL-12, IL-6 and IL-4induced large amounts of Blimp-1–GFP (**Supplementary Fig. 4b**,**c**). These data indicate that IL-2 and proinflammatory cytokines can induce *Blimp1* expression in natural T_{reg} cells and that Blimp-1$^+$ T_{reg} cells are the functionally mature effector cells of this lineage.

IRF4 is required for the generation of effector T_{reg} cells

The Blimp-1$^+$ T_{reg} population was enriched for both IRF4 and T-bet (**Fig. 2d**). Although IRF4 is required for the activation of *Blimp1* expression during plasma cell differentiation[36], the relationship between T-bet and Blimp-1 is unclear. To determine whether T-bet was necessary for the generation of Blimp-1$^+$ effector T_{reg} cells, we used *Tbx21*$^{-/-}$*Blimp1*$^{+/GFP}$ mice. T-bet was not essential for the differentiation of Blimp-1-expressing effector T_{reg} cells, for their expression of ICOS, CD103 or CD62L or for their tissue distribution (**Fig. 5a** and **Supplementary Fig. 5a–c**). Notably, however, Blimp-1–GFP$^+$ T_{reg} cells were absent from *Irf4*$^{-/-}$*Blimp1*$^{+/GFP}$ mice (**Fig. 5b**). The lack of *Blimp1* expression in T_{reg} cells was lineage specific, as conventional effector-memory CD4$^+$ T cells (CD25^{lo}CD44$^+$CD62L$^-$) had normal expression of Blimp-1–GFP (**Fig. 5b** and data not shown). Chromatin immunoprecipitation (ChIP) analysis of purified T_{reg} cells showed that IRF4 bound strongly to two previously identified binding sites in the 3′ region[37] and between exons 5 and 6 of *Blimp1* (conserved noncoding sequence 9)[36] (**Fig. 5c**), which indicated that IRF4 directly regulated *Blimp1* expression in T_{reg} cells.

IRF4 is required for the function of conventional T cells and T_{reg} cells during T_H2 responses[17]. Furthermore, IRF4-deficient mice have a series of additional immune deficiencies, including impaired T_H17 and T_H9 differentiation[38–40]. To determine if the absence of Blimp-1–GFP$^+$ IRF4-deficient T_{reg} cells was intrinsic to T_{reg} cells, we generated mixed chimeric mice generated with wild-type and *Irf4*$^{-/-}$ bone marrow. In agreement with a published report[17], *Irf4*$^{-/-}$ T_{reg} cells lacked ICOS expression (**Fig. 5d**); however, they also showed impaired CD62L downregulation and diminished expression of

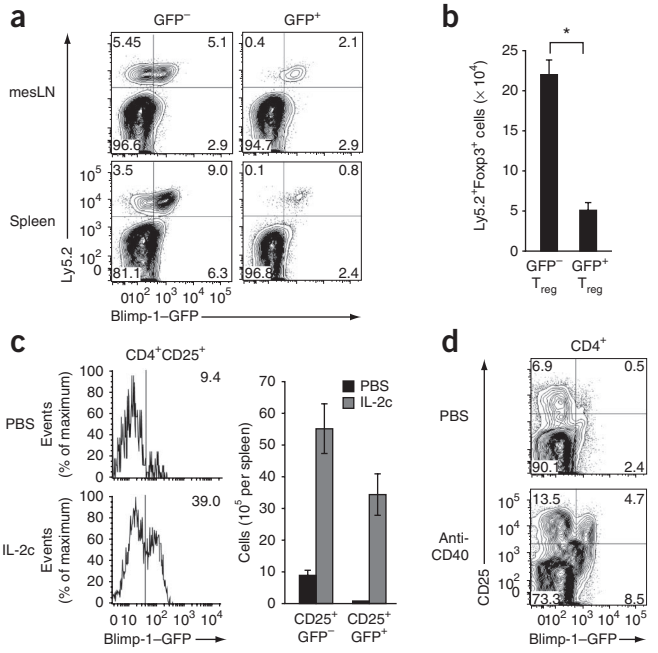

Figure 4 Blimp-1 limits numbers of T_{reg} cells and is induced by IL-2 and inflammatory signals. (**a**,**b**) GFP expression in CD4$^+$ T cells (**a**) and number of Ly5.2$^+$CD4$^+$ T cells (**b**) in the spleens of *Rag1*$^{-/-}$ Ly5.1$^+$ mice 8 weeks after transfer of CD4$^+$CD25$^-$CD62L$^+$ T cells, isolated from wild-type (Ly5.1$^+$) mice, plus either GFP$^-$ or GFP$^+$ CD4$^+$CD25$^+$ T cells, sorted from *Blimp1*$^{+/GFP}$(Ly5.2$^+$) mice. **P* = 0.002 (*t*-test). (**c**) Blimp-1–GFP expression in CD4$^+$CD25$^+$ T cells (left) and number of GFP$^+$ and GFP$^-$CD4$^+$CD25$^+$ T cells (right) in the spleen 7 d after injection of PBS or IL-2–anti-IL-2 complexes (IL-2c) into *Blimp1*$^{+/GFP}$ mice. Numbers in plots indicate percent Blimp-1–GFP$^+$ cells. (**d**) Flow cytometry of CD4$^+$ T cells on day 5 after injection of PBS or monoclonal anti-CD40 or PBS into *Blimp1*$^{+/GFP}$ mice on days 0, 2 and 4. Numbers in quadrants (**a**,**d**) indicate percent cells in each. Data are representative of three independent experiments with similar results with three mice per group (**a**,**b**; mean and s.e.m. in **b**) or two independent experiments with similar results, with one to two mice per group (PBS) or two to three mice per group (IL-2–anti-IL-2 or anti-CD40; **c**,**d**; mean ± s.d. in **c**).

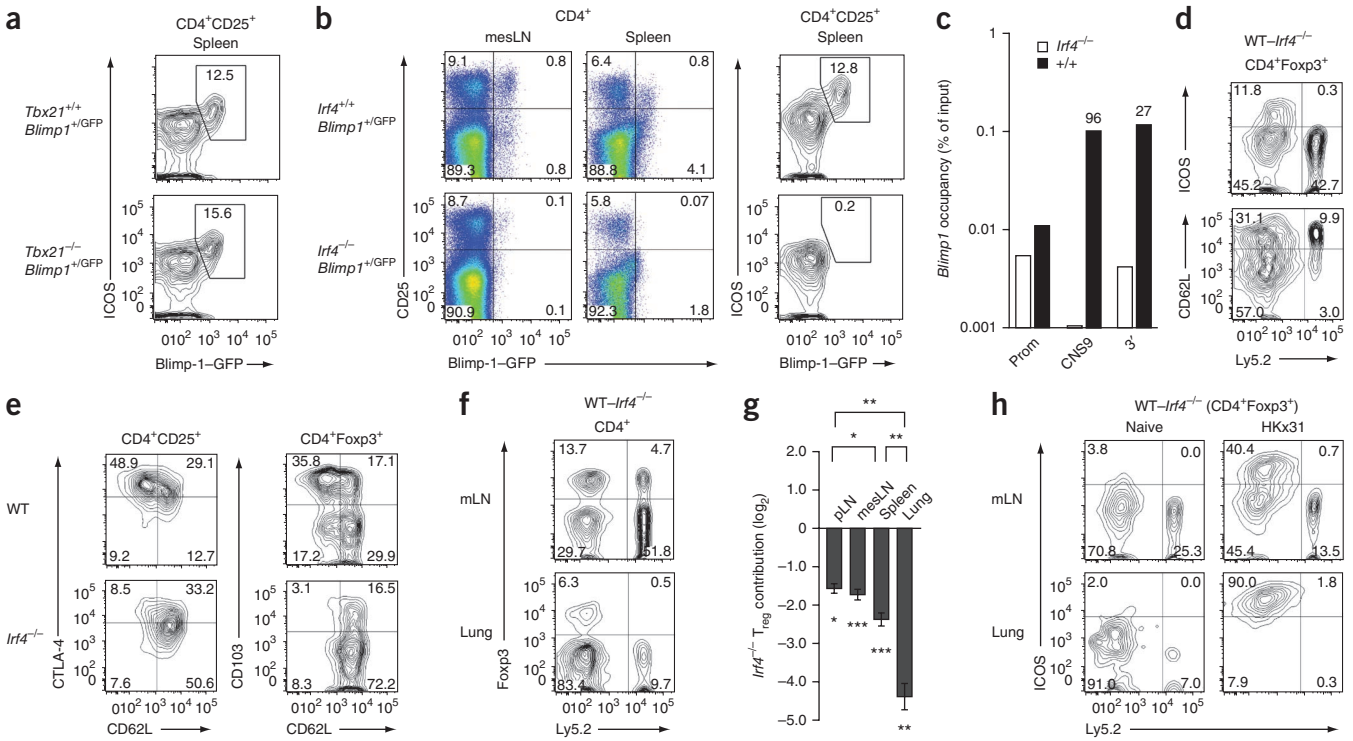

Figure 5 IRF4 is required for the generation of Blimp-1-expressing effector T_{reg} cells, but T-bet is not. (**a**,**b**) Flow cytometry of CD4$^+$ T cells from the spleens and mesenteric lymph nodes of *Tbx21*$^{-/-}$*Blimp1*$^{+/GFP}$ mice (**a**) or *Irf4*$^{-/-}$*Blimp1*$^{+/GFP}$ mice (**b**) and their respective littermate controls. (**c**) ChIP analysis of purified T_{reg} cells with an IRF4-specific antibody and PCR primers specific for the following regulatory regions of *Blimp1*: promoter (Prom), conserved noncoding sequence (CNS) and region 3′ to *Blimp1* (3′). Numbers above bars indicate enrichment relative to results obtained with the *Irf4*$^{-/-}$ control. (**d**–**f**) Flow cytometry of T_{reg} cells and CD4$^+$ T cells from the mesenteric lymph nodes (**d**,**e**) and mediastinal lymph nodes and lungs (**f**) of wild-type (Ly5.1$^+$)–*Irf4*$^{-/-}$ (Ly5.2$^+$) mixed–bone marrow chimeras (WT–*Irf4*$^{-/-}$). (**g**) Contribution of IRF4-deficient T_{reg} cells to various tissues in wild-type–*Irf4*$^{-/-}$ chimeric mice, presented as the ratio of Ly5.2$^+$CD4$^+$Foxp3$^+$ T cells to Ly5.2$^-$CD4$^+$Foxp3$^+$ T cells. $^*P < 0.01$, $^{**}P < 0.001$ and $^{***}P < 0.0001$ (*t*-test). (**h**) Flow cytometry of CD4$^+$Foxp3$^+$ T cells from mediastinal lymph nodes and lungs before and 10 d after infection of wild-type–*Irf4*$^{-/-}$ chimeric mice with influenza virus (strain HKx31). Numbers in outlined areas or quadrants (**a**,**b**,**d**,**e**,**f**,**h**) indicate percent cells in each. Data are representative of two to three experiments with two to three mice in each (**a**,**b**,**d**,**e**), three independent experiments (**c**) or two independent experiments with three to five mice per group (**f**–**h**; mean and s.e.m. in **g**).

CD103 and CTLA-4 (**Fig. 5d**,**e**), which suggested that the differentiation of effector T_{reg} cells was blocked in the absence of IRF4.

We next examined the distribution of wild-type and *Irf4*$^{-/-}$ T_{reg} cells in mixed–bone marrow chimeras. *Irf4*$^{-/-}$ T_{reg} cells were only slightly less abundant in lymphoid organs; however, they were almost completely absent from mucosal sites such as the lungs (**Fig. 5f**,**g**). To determine if inflammation would be sufficient to induce the acquisition of an effector phenotype in IRF4-deficient T_{reg} cells and their recruitment to mucosal sites, we infected wild-type–*Irf4*$^{-/-}$ mixed–bone marrow chimeras with influenza virus and examined T_{reg} cells in the lungs and draining lymph nodes at the peak of the response. Although wild-type T_{reg} cells upregulated ICOS and were efficiently recruited to the lung, *Irf4*$^{-/-}$ T_{reg} cells did not express ICOS and did not migrate to the lung (**Fig. 5h**). In addition, *Irf4*$^{-/-}$ T_{reg} cell did not express the differentiation marker KLRG1 (**Supplementary Fig. 6a**), which indicated that IRF4-deficient T_{reg} cells were unable to acquire an effector phenotype even in the presence of activation signals.

Our data suggested that IRF4 was not only involved in T_{reg} cell differentiation during T_H2-type immune responses[17] but also required during in T_H1-type inflammatory conditions, such as viral infection. To examine this possibility in detail, we labeled T_{reg} cells from wild-type–*Irf4*$^{-/-}$ mixed–bone marrow chimeras with the cytosolic dye CFSE and transferred the cells into recipients deficient in the signal-transduction molecule CD3ε, in which T_H1 inflammation and T_{reg} cell activation are induced by injection of anti-CD40 (ref. 18). At 6 d after transfer, both wild-type and *Irf4*$^{-/-}$Foxp3$^+$ T_{reg} cells had proliferated extensively. Most wild-type Foxp3$^+$ cells had lost CD62L expression and upregulated T-bet (**Supplementary Fig. 6b**), indicative of T_{reg} cell differentiation under T_H1 conditions. *Irf4*$^{-/-}$ T_{reg} cells, however, were considerably impaired in CD62L downregulation and almost completely lacked T-bet expression. Consistent with the observation that Blimp-1 is not required for the generation of effector T_{reg} cells, Blimp-1-deficient T_{reg} cells isolated from mice with *lox*P-flanked *Blimp1* alleles, with expression of Cre recombinase from the promoter of the gene encoding the kinase Lck[31], downregulated CD62L and expressed normal amounts of T-bet, similar to wild-type T_{reg} cells (**Supplementary Fig. 6b**). These results suggest that IRF4 is required for the differentiation of all effector T_{reg} cells.

Coregulation of effector T_{reg} cell function by Blimp-1 and IRF4

To identify genes whose expression in T_{reg} cells was deregulated in the absence of Blimp-1, we sorted Blimp-1–GFP$^+$ T_{reg} cells from *Blimp1*$^{+/GFP}$ and *Blimp1*$^{GFP/GFP}$ mice and subjected them to microarray analysis. We found 758 unique genes with differences in expression in the two populations (**Fig. 6a**, **Supplementary Table 1** and data not shown). Quantitative real-time PCR as well as flow cytometry confirmed the differences in expression of a panel of selected genes (**Fig. 6b**–**d**), including known Blimp-1 target genes such as *Id3* and

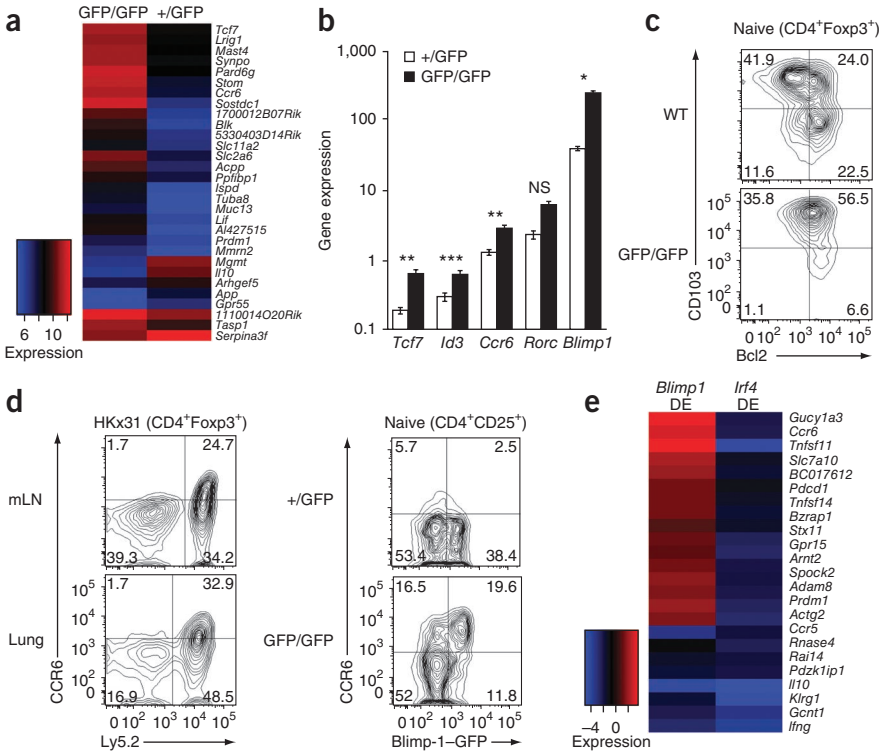

Figure 6 Blimp-1 and IRF4 jointly regulate the effector T_{reg} cell differentiation program. (**a**) Microarray analysis of Blimp-1–GFP$^+$ T_{reg} cells isolated from the *Blimp1*$^{GFP/GFP}$ or *Blimp1*$^{+/GFP}$ compartment of bone–marrow chimeric mice, presented as a heat map of the 30 genes with the greatest differences in expression (presented as normalized intensity (log_2)). Data are from three experiments (mean). (**b**) Quantitative RT-PCR analysis of gene expression in T_{reg} cell populations from *Blimp1*$^{+/GFP}$ and *Blimp1*$^{GFP/GFP}$ mice, presented as expression in Blimp-1–GFP$^+$ cells relative to that in Blimp-1–GFP$^-$ T_{reg} cells. NS, not significant ($P = 0.13$); $^*P = 0.03$, $^{**}P = 0.02$ and $^{***}P = 0.01$ (*t*-test). Data are representative of three experiments (mean ± s.d. of three biological replicates). (**c**,**d**) Flow cytometry of T_{reg} cells from wild-type (Ly5.1$^+$)–*Blimp1*$^{GFP/GFP}$ (Ly5.2$^+$) or wild-type (Ly5.1$^+$)–*Blimp1*$^{+/GFP}$ (Ly5.2$^+$) mixed–bone marrow chimeras before or after infection with influenza virus (strain HKx31); cell gating, above plots; genotype or organ, left margins. Numbers in quadrants indicate percent cells in each. Data are representative of three experiments with two to three mice each. (**e**) Comparative analysis of genes with different expression (DE) in the Blimp-1 data set (*Blimp1*$^{GFP/GFP}$ and *Blimp1*$^{+/GFP}$ mice) and the IRF4 data set (mice expressing Cre recombinase from the *Foxp3* promoter, with *lox*P-flanked (fl) alleles: *Irf4*$^{-/fl}$ and *Irf4*$^{+/fl}$); results are presented as normalized intensity (log_2) relative to those of wild-type mice. Data are from three (*Blimp1* DE) or two (*Irf4* DE) experiments (mean).

Blimp1 itself[41,42]. Among the genes with differences in expression, the genes encoding Bcl-2 and the chemokine receptor CCR6 were significantly upregulated in Blimp-1-deficient T_{reg} cells as both mRNA ($P = 0.0002$ and $P = 0.0000003$, respectively) and protein (**Fig. 6a–d** and **Supplementary Fig. 7a**), a finding that could explain the accumulation of Blimp-1-deficient effector T_{reg} cells in nonlymphoid tissues. In line with that conclusion, the proliferation of Blimp-1-deficient T_{reg} cells was not markedly altered (**Supplementary Fig. 7b**), and Blimp-1–GFP$^+$ T_{reg} cells accumulated significantly in mice deficient in the proapoptotic Bcl-2 family member Bim ($P = 0.0006$; **Supplementary Fig. 7c,d**), which suggested that the balance of prosurvival and proapoptotic proteins regulates the survival of effector T_{reg} cells.

To identify the individual contributions of Blimp-1 and IRF4 to the differentiation of effector T_{reg} cells, we compared our microarray analysis with previously identified IRF4-dependent genes in T_{reg} cells[17]. In both the Blimp-1 and IRF4 data sets, there was significant enrichment for genes with differences in expression ($P = 5 \times 10^{-16}$), including *Il10*, *Klrg1*, *Ebi3*, *Ccr6*, *Bcl2, Rorc* and *Blimp1* (**Fig. 6e** and **Supplementary Fig. 8a,b**). Most of these genes required IRF4 for their expression ($P = 0.006$; **Fig. 6e**, **Supplementary Fig. 8a,b** and **Supplementary Table 2**), and their expression was very different in Blimp-1–GFP$^-$ and Blimp-1–GFP$^+$ T_{reg} cells (**Supplementary Fig. 8c–e**), which indicated a distinct differentiation program that requires both IRF4 and Blimp-1. In support of that idea, overexpression of Blimp-1 alone was not sufficient to restore the effector differentiation of IRF4-deficient T_{reg} cells (**Supplementary Fig. 9**).

Published studies have identified conserved noncoding DNA sequences and promoter elements important for the IRF4-mediated regulation of *Il10* expression in conventional T cells[43,44]; furthermore, our computational analysis showed the presence of putative IRF4-binding sites in the first introns of *Il10* and *Ccr6*. ChIP analysis confirmed strong binding of IRF4 to these elements (**Fig. 7a**), which indicated that IRF4 directly regulates the expression of *Il10* and *Ccr6* in T_{reg} cells. We detected prominent acetylation of histone H3 at Lys9 and trimethylation of histone H3 at Lys4, consistent with active transcription, in these elements in the *Il10* locus in wild-type T_{reg} cells but not in IRF4-deficient T_{reg} cells. Conversely, trimethylation of histone H3 at Lys27, an inhibitory modification, was overrepresented in the *Il10* promoter region in IRF4-deficient T_{reg} cells. Blimp-1-deficient T_{reg} cells, however, lacked such trimethylation and had fewer activating histone marks (**Fig. 7b**) despite the unchanged binding of IRF4 to these sites (**Supplementary Fig. 10**). These results indicate that both Blimp-1 and IRF4 are required for the remodeling of active chromatin at the *Il10* locus.

Computational analysis of intron 1 of *Il10* showed the presence of several putative Blimp-1-binding sites, two of which were conserved between mice and humans (**Supplementary Fig. 11**). To investigate whether Blimp-1 was able to bind to this region *in vivo*, we did antibody-independent ChIP analysis of Blimp-1 by taking advantage of *Blimp1*$^{Bio/Bio}$*Rosa26*$^{BirA/BirA}$ mice, which express biotinylated Blimp-1 in all *Blimp1*-expressing cells (M.M. and M.B., unpublished data). By streptavidin-mediated ChIP and quantitative PCR analysis of T_{reg} cells, we detected binding of Blimp-1 specifically in intron 1 of *Il10* (**Fig. 7c**). Binding of Blimp-1 was undetectable in control sequences located in the 3′ region of the B cell–specific gene *Cd19* or when assessed by ChIP with control immunoglobulin G beads. These results demonstrate that Blimp-1 binds specifically in intron 1 of the *Il10* locus and, together with IRF4, directly regulates *Il10* expression in T_{reg} cells. Collectively, these data suggest a model in which IRF4 is essential for effector T_{reg} cell differentiation, whereas Blimp-1 is required for their functional maturation (**Supplementary Fig. 12**).

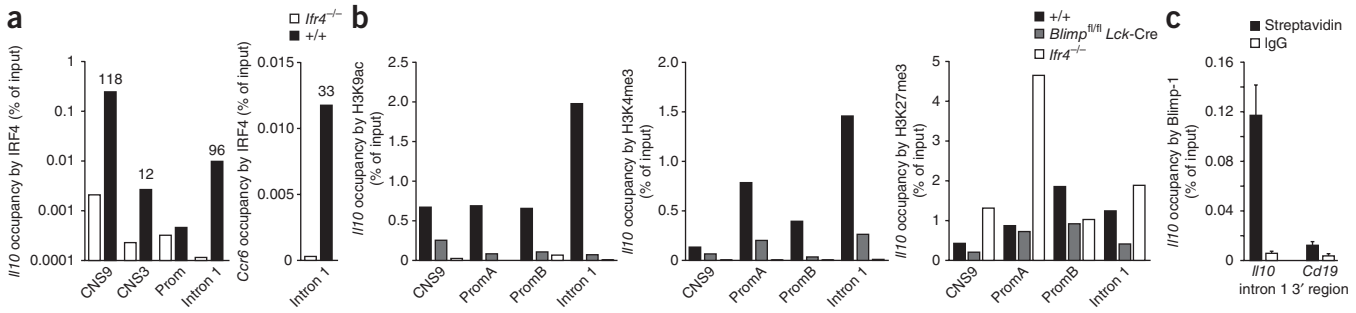

Figure 7 Binding of IRF4 and Blimp-1 to regulatory regions in the *Il10* and *Ccr6* loci. (**a**) ChIP analysis of purified *Irf4*$^{-/-}$ and *Irf4*$^{+/+}$ T_{reg} cells, assessed with an IRF4-specific antibody and PCR primers specific for regulatory regions of *Il10* and *Ccr6*. Numbers above bars indicate enrichment relative to that in *Irf4*$^{-/-}$ T cells. (**b**) ChIP analysis of the *Il10* locus with antiserum specific for acetylation of histone H3 at Lys9 (H3K9ac) or trimethylation of histone H3 at Lys4 (H3K4me3) or Lys27 (H3K27me3). (**c**) Binding of Blimp-1 to intron 1 of *Il10*, analyzed by streptavidin-mediated ChIP analysis of *in vitro*–activated T_{reg} cells from *Blimp1*$^{Bio/Bio}$ *Rosa26*$^{BirA/BirA}$ mice. Input DNA and precipitated DNA were quantified by real-time PCR with primer pairs amplifying a conserved sequence in *Il10* intron 1 or a control sequence in the 3′ region of *Cd19*; the same chromatin was used for control ChIP experiments with immunoglobulin G–coupled Dynabeads. Precipitated DNA is presented relative to input DNA. Data are representative of three to four independent experiments (**a**,**b**) or two independent experiments (**c**; mean and s.d.).

DISCUSSION

Functional diversification is well known for conventional CD4$^+$ T cells. However, it is now realized that unexpected phenotypic and functional diversity of T_{reg} cells exists, driven by transcription factors distinct from Foxp3 (ref. 45). Notably, the production of IL-10 by T_{reg} cells occurs in a variety of different conditions, which raises the possibility that these T_{reg} cell subsets use a common differentiation program. Here we have identified Blimp-1 as the transcription factor required for IL-10 production and tissue homeostasis of T_{reg} cells and have demonstrated a broader role than previously proposed for IRF4 in the differentiation of effector T_{reg} cells.

Despite the fact that Blimp-1 has been linked to T_{reg} cell function before[25,26], its role in this lineage has remained elusive. We have demonstrated here that Blimp-1 expression in T_{reg} cells was restricted to a distinct population of cells with an effector phenotype that produced large quantities of IL-10, had high expression of ICOS, tended to localize to nonlymphoid tissues and thus represented the counterparts of the ICOS$^+$IL-10$^+$ T_{reg} cells described in humans[12]. Blimp-1 was dispensable for the differentiation of effector-phenotype T_{reg} cells but it was absolutely required for IL-10 expression, for the upregulation of ICOS after activation and for the homeostasis of T_{reg} cells, in particular at mucosal surfaces and tissues. Our findings are in line with the similarities in the disease pathology of Blimp-1-deficient mice and mice with T_{reg} cell–specific *Il10* deficiency and suggest that the lack of IL-10 production by T_{reg} cells is the main contributor to the pathology of Blimp-1-deficient mice[11,25]. Our data have further demonstrated that Blimp-1 restricted the number of effector T_{reg} cells at environmental interfaces such as the gastrointestinal tract and the lungs. This seemed to be mediated by limitation of the expression of Bcl-2 and of CCR6, which mediates the migration of T_H17 cells and T_{reg} cells to inflammatory sites and nonlymphoid tissues[13,46,47].

IL-2 has a central role in T_{reg} cell biology. Foxp3 directly regulates high expression of the IL-2 receptor α-chain (CD25), and signals from the IL-2 receptor complex are required for the survival of peripheral T_{reg} cells[3,4,6]. Here we have shown that IL-2, together with inflammatory cytokines, induced *Blimp1* expression. Natural T_{reg} cells upregulated *Blimp1* expression during active suppression *in vivo*, which suggested that Blimp-1 provides a common molecular signature for T_{reg} cells 'in action' regardless of their location and polarization.

IRF4 is important for plasma cell differentiation[36,38,48] and induces *Blimp1* expression during this process[36]. We found that IRF4-deficient T_{reg} cells failed to differentiate into effector T_{reg} cells and lacked *Blimp1* expression and that IRF4 directly activated *Blimp1* expression, thus demonstrating that IRF4 acts upstream of Blimp-1 in the differentiation of effector T_{reg} cells. IRF4-deficient T_{reg} cells not only lacked ICOS expression and IL-10 production but also were impaired in the regulation of activation markers and molecules required for homing, such as CD62L, CD103 and CCR6, and suppressor function, such as CTLA-4. IRF4 is required for the suppression of T_H2-driven autoimmunity by T_{reg} cells[17]. Notably, our experiments showed that *Irf4*$^{-/-}$ T_{reg} cells failed to upregulate T-bet under T_H1 inflammatory conditions, which demonstrated that IRF4 is required for the differentiation of effector T_{reg} cells not only in T_H2 environments but also in T_H1 environments. We therefore propose a broader role for IRF4 in the differentiation of all effector T_{reg} cells.

The degree to which IRF4 and Blimp-1 act together in the differentiation of effector T_{reg} cells was demonstrated by comparative analysis of our microarray results and published microarray data[17]. Among the probes with differences in expression in wild-type and Blimp-1-deficient T_{reg} cells, we found significant enrichment for genes that required IRF4 for their expression. These genes included most prominently *Il10*, which we found to be a direct target of IRF4 in T_{reg} cells. Examination of the histone marks of the *Il10* locus provided evidence for distinct effects of IRF4 and Blimp-1 on this gene. Whereas IRF4 functioned to prime the *Il10* regulatory regions by removing repressive trimethylation of histone H3 at Lys27 before active transcription, Blimp-1 was required for the normal deposition of active chromatin marks. Although Blimp-1 has been reported to act only as a transcriptional repressor[24], its direct binding to a conserved region in intron 1 of *Il10* raises the possibility that it also has a positive role in gene expression. Future molecular work should examine in detail how Blimp-1 can act as both a suppressor and an activator of gene expression.

The relationship between Blimp-1 and T-bet is less clear. T-bet-deficient T_{reg} cells had expression normal of Blimp-1–GFP and ICOS, which suggested that T-bet is not required for the formation of effector T_{reg} cells. Furthermore, T-bet expression in Blimp-1-deficient T_{reg} cells was similar to that in their wild-type counterparts, in both naive and T_H1 inflammatory conditions, which suggests that T-bet and Blimp-1 do not regulate each other's expression in T_{reg} cell differentiation.

The idea that Foxp3$^+$ T_{reg} cells undergo a differentiation and specialization program in the periphery analogous to that of conventional CD4$^+$ T cells is clinically important, as modulation of T_{reg} cell function is of great interest in many medical conditions[45]. The proposal that naive T_{reg} cells differ from differentiated effector T_{reg} cells suggests that in conditions such as autoimmunity, organ transplantation

or cancer, the critical parameters that control immune responses may be not only the number of T_{reg} cells but also their acquisition of an effector phenotype. Understanding the factors that guide the differentiation program of effector T_{reg} cells is essential in considering the therapeutic potential of IL-2 complex–induced or transforming growth factor-β-induced T_{reg} cells or in assessing the success of strategies that inhibit or delete T_{reg} cells. In this study, we have defined some of the critical molecular requirements for effector T_{reg} cells and have identified extrinsic signals crucial for regulation of this population. Our data have shown that IL-2 and inflammatory signals and two conserved transcription factors, IRF4 and Blimp-1, jointly regulate the differentiation, function and homeostasis of effector T_{reg} cells.

METHODS

Methods and any associated references are available in the online version of the paper at http://www.nature.com/natureimmunology/.

Accession codes. GEO: *Blimp1* microarray data, GSE27143.

Note: Supplementary information is available on the Nature Immunology website.

ACKNOWLEDGMENTS

We thank T. Mak, L. Wu, J. Altin and P. Bouillet for mice; S. Sterle, N. Bernard, R. Thong and K. Elder for technical support; Y. Zhan, I. Campbell and K. Shortman for antibodies; L. Corcoran and D. Tarlinton for discussion and reagents; and Y. Zheng and A. Rudensky for the full microarray data set already published in part[17]. Supported by the National Health and Medical Research Council of Australia (E.C., G.T.B., S.L.N. and A.K.), L'Oréal Australia For Women in Science Fellowship (E.C.), the Swiss National Science Foundation (F.M.), the Viertel Foundation, the Howard Hughes Medical Institute (G.T.B.), the Pfizer Australia Research Fellowship program (S.L.N.), the Leukemia & Lymphoma Society (A.K.), Boehringer Ingelheim (Busslinger group) and the European Union Sixth Framework Programme FP6 (EuTRACC project, Busslinger group).

AUTHOR CONTRIBUTIONS

E.C., A.X., M.M., F.M., M.M. and A.K. designed and did experiments; W.S. and G.K.S. analyzed the microarray data; G.T.B. and M.B. designed experiments; and S.L.N. and A.K. designed experiments and wrote the paper and contributed equally to this work.

COMPETING FINANCIAL INTERESTS

The authors declare no competing financial interests.

Published online at http://www.nature.com/natureimmunology/.
Reprints and permissions information is available online at http://npg.nature.com/reprintsandpermissions/.

1. Lu, L.F. & Rudensky, A. Molecular orchestration of differentiation and function of regulatory T cells. *Genes Dev.* **23**, 1270–1282 (2009).
2. Sakaguchi, S., Yamaguchi, T., Nomura, T. & Ono, M. Regulatory T cells and immune tolerance. *Cell* **133**, 775–787 (2008).
3. D'Cruz, L.M. & Klein, L. Development and function of agonist-induced CD25$^+$Foxp3$^+$ regulatory T cells in the absence of interleukin 2 signaling. *Nat. Immunol.* **6**, 1152–1159 (2005).
4. Fontenot, J.D., Rasmussen, J.P., Gavin, M.A. & Rudensky, A.Y. A function for interleukin 2 in Foxp3-expressing regulatory T cells. *Nat. Immunol.* **6**, 1142–1151 (2005).
5. Zheng, Y. & Rudensky, A.Y. Foxp3 in control of the regulatory T cell lineage. *Nat. Immunol.* **8**, 457–462 (2007).
6. Fontenot, J.D., Gavin, M.A. & Rudensky, A.Y. Foxp3 programs the development and function of CD4$^+$CD25$^+$ regulatory T cells. *Nat. Immunol.* **4**, 330–336 (2003).
7. Fontenot, J.D. *et al.* Regulatory T cell lineage specification by the forkhead transcription factor foxp3. *Immunity* **22**, 329–341 (2005).
8. Wing, K. *et al.* CTLA-4 control over Foxp3$^+$ regulatory T cell function. *Science* **322**, 271–275 (2008).
9. Friedline, R.H. *et al.* CD4$^+$ regulatory T cells require CTLA-4 for the maintenance of systemic tolerance. *J. Exp. Med.* **206**, 421–434 (2009).
10. Pandiyan, P., Zheng, L., Ishihara, S., Reed, J. & Lenardo, M.J. CD4$^+$CD25$^+$Foxp3$^+$ regulatory T cells induce cytokine deprivation-mediated apoptosis of effector CD4$^+$ T cells. *Nat. Immunol.* **8**, 1353–1362 (2007).
11. Rubtsov, Y.P. *et al.* Regulatory T cell-derived interleukin-10 limits inflammation at environmental interfaces. *Immunity* **28**, 546–558 (2008).
12. Ito, T. *et al.* Two functional subsets of FOXP3$^+$ regulatory T cells in human thymus and periphery. *Immunity* **28**, 870–880 (2008).
13. Kleinewietfeld, M. *et al.* CCR6 expression defines regulatory effector/memory-like cells within the CD25$^+$CD4$^+$ T-cell subset. *Blood* **105**, 2877–2886 (2005).
14. Strauss, L. *et al.* Expression of ICOS on human melanoma-infiltrating CD4$^+$CD25^{high}Foxp3$^+$ T regulatory cells: implications and impact on tumor-mediated immune suppression. *J. Immunol.* **180**, 2967–2980 (2008).
15. Zhang, N. *et al.* Regulatory T cells sequentially migrate from inflamed tissues to draining lymph nodes to suppress the alloimmune response. *Immunity* **30**, 458–469 (2009).
16. Kamanaka, M. *et al.* Expression of interleukin-10 in intestinal lymphocytes detected by an interleukin-10 reporter knockin tiger mouse. *Immunity* **25**, 941–952 (2006).
17. Zheng, Y. *et al.* Regulatory T-cell suppressor program co-opts transcription factor IRF4 to control T_H2 responses. *Nature* **458**, 351–356 (2009).
18. Koch, M.A. *et al.* The transcription factor T-bet controls regulatory T cell homeostasis and function during type 1 inflammation. *Nat. Immunol.* **10**, 595–602 (2009).
19. Chaudhry, A. *et al.* CD4$^+$ regulatory T cells control T_H17 responses in a Stat3-dependent manner. *Science* **326**, 986–991 (2009).
20. Gavin, M.A. *et al.* Foxp3-dependent programme of regulatory T-cell differentiation. *Nature* **445**, 771–775 (2007).
21. Zheng, Y. *et al.* Genome-wide analysis of Foxp3 target genes in developing and mature regulatory T cells. *Nature* **445**, 936–940 (2007).
22. Nutt, S.L., Fairfax, K.A. & Kallies, A. BLIMP1 guides the fate of effector B and T cells. *Nat. Rev. Immunol.* **7**, 923–927 (2007).
23. Kallies, A. & Nutt, S.L. Terminal differentiation of lymphocytes depends on Blimp-1. *Curr. Opin. Immunol.* **19**, 156–162 (2007).
24. Martins, G. & Calame, K. Regulation and functions of Blimp-1 in T and B lymphocytes. *Annu. Rev. Immunol.* **26**, 133–169 (2008).
25. Kallies, A. *et al.* Transcriptional repressor Blimp-1 is essential for T cell homeostasis and self-tolerance. *Nat. Immunol.* **7**, 466–474 (2006).
26. Martins, G.A. *et al.* Transcriptional repressor Blimp-1 regulates T cell homeostasis and function. *Nat. Immunol.* **7**, 457–465 (2006).
27. Gong, D. & Malek, T.R. Cytokine-dependent Blimp-1 expression in activated T cells inhibits IL-2 production. *J. Immunol.* **178**, 242–252 (2007).
28. Santer-Nanan, B. *et al.* Blimp-1 is expressed in human and mouse T cell subsets and leads to loss of IL-2 production and to defective proliferation. *Signal Transduct.* **6**, 268–279 (2006).
29. Cimmino, L. *et al.* Blimp-1 attenuates Th1 differentiation by repression of ifng, tbx21, and bcl6 gene expression. *J. Immunol.* **181**, 2338–2347 (2008).
30. Johnston, R.J. *et al.* Bcl6 and Blimp-1 are reciprocal and antagonistic regulators of T follicular helper cell differentiation. *Science* **325**, 1006–1010 (2009).
31. Kallies, A., Xin, A., Belz, G.T. & Nutt, S.L. Blimp-1 transcription factor is required for the differentiation of effector CD8$^+$ T cells and memory responses. *Immunity* **31**, 283–295 (2009).
32. Rutishauser, R.L. *et al.* Transcriptional repressor Blimp-1 promotes CD8$^+$ T cell terminal differentiation and represses the acquisition of central memory T cell properties. *Immunity* **31**, 296–308 (2009).
33. Kallies, A. *et al.* Plasma cell ontogeny defined by quantitative changes in blimp-1 expression. *J. Exp. Med.* **200**, 967–977 (2004).
34. Mottet, C., Uhlig, H.H. & Powrie, F. Cutting edge: cure of colitis by CD4$^+$CD25$^+$ regulatory T cells. *J. Immunol.* **170**, 3939–3943 (2003).
35. Boyman, O., Kovar, M., Rubinstein, M.P., Surh, C.D. & Sprent, J. Selective stimulation of T cell subsets with antibody-cytokine immune complexes. *Science* **311**, 1924–1927 (2006).
36. Sciammas, R. *et al.* Graded expression of interferon regulatory factor-4 coordinates isotype switching with plasma cell differentiation. *Immunity* **25**, 225–236 (2006).
37. Kwon, H. *et al.* Analysis of interleukin-21-induced Prdm1 gene regulation reveals functional cooperation of STAT3 and IRF4 transcription factors. *Immunity* **31**, 941–952 (2009).
38. Mittrucker, H.W. *et al.* Requirement for the transcription factor LSIRF/IRF4 for mature B and T lymphocyte function. *Science* **275**, 540–543 (1997).
39. Brustle, A. *et al.* The development of inflammatory T_H-17 cells requires interferon-regulatory factor 4. *Nat. Immunol.* **8**, 958–966 (2007).
40. Staudt, V. *et al.* Interferon-regulatory factor 4 is essential for the developmental program of T helper 9 cells. *Immunity* **33**, 192–202 (2010).
41. Shaffer, A.L. *et al.* Blimp-1 orchestrates plasma cell differentiation by extinguishing the mature B cell gene expression program. *Immunity* **17**, 51–62 (2002).
42. Magnusdottir, E. *et al.* Epidermal terminal differentiation depends on B lymphocyte-induced maturation protein-1. *Proc. Natl. Acad. Sci. USA* **104**, 14988–14993 (2007).
43. Lee, C.G. *et al.* A distal *cis*-regulatory element, CNS-9, controls NFAT1 and IRF4-mediated IL-10 gene activation in T helper cells. *Mol. Immunol.* **46**, 613–621 (2009).
44. Ahyi, A.N., Chang, H.C., Dent, A.L., Nutt, S.L. & Kaplan, M.H. IFN regulatory factor 4 regulates the expression of a subset of Th2 cytokines. *J. Immunol.* **183**, 1598–1606 (2009).
45. Campbell, D.J. & Koch, M.A. Phenotypical and functional specialization of FOXP3$^+$ regulatory T cells. *Nat. Rev. Immunol.* **11**, 119–130 (2011).
46. Yamazaki, T. *et al.* CCR6 regulates the migration of inflammatory and regulatory T cells. *J. Immunol.* **181**, 8391–8401 (2008).
47. Kitamura, K., Farber, J.M. & Kelsall, B.L. CCR6 marks regulatory T cells as a colon-tropic, IL-10-producing phenotype. *J. Immunol.* **185**, 3295–3304 (2010).
48. Klein, U. *et al.* Transcription factor IRF4 controls plasma cell differentiation and class-switch recombination. *Nat. Immunol.* **7**, 773–782 (2006).

ONLINE METHODS

Mice. *Blimp1*$^{+/GFP}$ and *Blimp1*$^{fl/fl}$*Lck*-Cre mice were generated as described[31,33]. *Irf4*$^{-/-}$ mice[38], CD3ε-deficient mice[49], *Foxp3*$^{+/-}$ mice[6], *Bim*$^{-/-}$ mice[50] and *Tbx21*$^{-/-}$ mice[51] have been described. *Rag1*$^{-/-}$ mice were from The Jackson Laboratory. *Blimp1*$^{GFP/GFP}$ mice were generated as described[52]. The *Blimp1*$^{Bio/Bio}$ knock-in mouse (M.M. and M.B., unpublished data) carries a biotin acceptor sequence at the carboxyl terminus of Blimp-1, which was biotinylated *in vivo* by coexpression of the *Escherichia coli* biotin ligase BirA[53] from the *Rosa26*^{BirA} allele[54]. Wild-type–*Irf4*$^{-/-}$ or wild-type–*Blimp1*$^{GFP/GFP}$ mixed–bone marrow chimeras were generated by reconstitution of lethally irradiated Ly5.1^{+} recipients with a mixture of bone marrow cells isolated from wild-type (Ly5.1^{+}) mice and *Irf4*$^{-/-}$ or *Blimp1*$^{GFP/GFP}$ (Ly5.2^{+}) mice. Chimeric mice were analyzed after a minimum of 6 weeks. To allow for variation in the reconstitution frequency, data were normalized for the proportion of the total CD4^{+} T cell compartment in the peripheral lymph nodes. All mice were bred and maintained on a C57BL/6 background at The Walter and Eliza Hall Institute of Medical Research. Animal experiments were done according to Animal Experimental Ethics Committee guidelines and approval.

Antibodies and flow cytometry. The following monoclonal antibodies to mouse were used for multiparameter flow cytometry (all from BD Biosciences Pharmingen): phycoerythrin-indotricarbocyanine–anti-CD4 (L3T4), allophycocyanin–anti-CD8 (53-6.7), phycoerythrin–anti-CD25 (PC61), biotin–anti-CD25 (7D4), phycoerythrin–anti-Foxp3 (FJK-16s), allophycocyanin–anti-CD62L (MEL-14), fluorescein isothiocyanate–anti-Ly5.2, peridinin chlorophyll protein (PerCP)–cyanine 5.5–anti-Ly5.2 or allophycocyanin–anti-Ly5.2 (104), PerCP–cyanine 5.5–anti-Ly5.1 (A20), phycoerythrin-indodicarbocyanine–anti-ICOS or biotin–anti-ICOS (7E.17G9), PerCP–cyanine 5.5–anti-IL7R (A7R34), phycoerythrin–anti-CD44 (IM7), biotin–anti-GITR (DTA-1), biotin–anti-CD69 (H1.2F3), phycoerythrin–anti-CD103 (2E7), biotin–anti-CD103 (M290), biotin–anti-CD38 (NIM-R5), phycoerythrin–anti-CTLA-4 (JC10-4F10-11), fluoroscein isothiocyanate–anti-Ki67 (B56) and phycoerythrin–anti-Bcl-2 (3F11). Biotinylated monoclonal antibodies were visualized with streptavidin-indodicarbocyanine or streptavidin–PerCP–cyanine 5.5. A Foxp3-PE staining kit and phycoerythrin–anti-CD103 (M290), phycoerythrin-indotricarbocyanine–anti-CD4, PerCP–cyanine 5.5–anti-Ly5.1, phycoerythrin-indotricarbocyanine–anti-ICOS and PerCP–cyanine 5.5–anti-IL-7Rα were used according to the manufacturer's protocol (eBioscience). Mouse anti-T-bet (4B10; Santa Cruz) was visualized with allophycocyanin-conjugated antibody to immunoglobulin G1 (x56; BD Biosciences Pharmingen). The Foxp3 staining kit was used for staining for CTLA-4, T-bet, Ki67 (fluorescein isothiocyanate) and Bcl-2 (phycoerythrin). Streptavidin-indodicarbocyanine was from Southern Biotechnology, and phycoerythrin–anti-CCR6 (FAB590P) was from R&D Systems. Viable cells were identified by propidium iodide exclusion or SytoxBlue exclusion (Invitrogen). Cells were analyzed on an LSR II, FACSCalibur or FACSCanto (Becton Dickinson) and were sorted on a MoFlo (Becton Coulter) or FACSAria (Becton Dickinson). Data were processed with Flowjo and Weasel software.

Cell isolation and culture. Unless described otherwise, lymph node and splenic cells were isolated and pooled for cell sorting by flow cytometry. Samples were pre-enriched for CD4^{+}CD25^{+} cells (pooled from spleen and lymph nodes) by magnetic-activated cell sorting with biotin–anti-CD25 and anti-biotin MACS beads according to the manufacturer's protocol (Miltenyi) and were subsequently sorted according to their Blimp-1–GFP expression to >96% purity. Cells were cultured for 7 d on plates coated with anti-CD3 (10 μg/ml; 145-2C11) in the presence of monoclonal anti-CD28 (2 μg/ml; 37.51) and recombinant mouse IL-2 (100 U/ml; R&D Systems) together with recombinant mouse IL-6 (20 ng/ml; eBioscience), recombinant mouse IL-4 (20 ng/ml; R&D Systems) or recombinant mouse IL-12 (5 ng/ml; R&D Systems). For ChIP experiments, T_{reg} cells were purified with a CD4^{+}CD25^{+} Regulatory T Cell Isolation kit (Miltenyi). Purity was between 93% and 95%. Lung lymphocytes were examined in bronchoalveolar lavage fluid.

Isolation of intraepithelial lymphocytes. Before isolation of intraepithelial lymphocytes, Peyer's patches were removed from the small intestine. The small intestine was then washed in Hanks2.5 medium (Hank's medium without calcium or magnesium, supplemented with 2.5% (vol/vol) FCS) and were cut in small pieces. Intraepithelial lymphocytes were separated from the intestine epithelial layer by successive incubation for 30 min at 25 °C in Hanks2.5 medium containing 1 mM dithiothreitol and then four times for 30 min each at 37 °C in Hanks2.5 medium containing 1 mM EDTA. The two fractions were combined and lymphocytes were further purified by centrifugation at 900*g* for 25 min at 25 °C on a Percoll density gradient (67–44%).

Cytokine assays. CD4^{+} T cells were sorted by flow cytometry from pooled spleen and lymph nodes from *Blimp1*$^{+/GFP}$ mice and were stimulated for 22–24 h with monoclonal anti-CD3 and anti-CD28. Supernatants were collected and assayed for cytokines with a Bioplex cytokine bead assay (Mouse 23-Plex Panel; Bio-Rad).

ChIP assays. For ChIP experiments, T_{reg} cells enriched by magnetic-activated cell sorting were cultured for 4 d as described above in the presence of IL-2 and IL-6. IRF4 was precipitated from 1.0×10^7 T_{reg} cells with 10 μg anti-IRF4 (M-17; Santa Cruz) as described[55]. *Irf4*$^{-/-}$ thymocytes served as a negative control. Histone ChIP analysis was done with monoclonal antibody to histone H3 trimethylated at Lys4 (17-614) and polyclonal antibody to histone H3 acetylated at Lys9 (07-352) or to histone H3 trimethylated at Lys27 (07-449; all from Millipore), with 0.5×10^6 to 1.0×10^6 T_{reg} cells per experiment. Quantitative PCR was used for analysis of enrichment (primers, **Supplementary Methods**). Standard curves were generated from serial dilutions of whole-cell extract DNA. Reactions were done in triplicate with SYBR Green PCR Master mix (Invitrogen) or GoTaq (Promega) on an ABI 7900HT. For chromatin precipitation by streptavidin, CD25^{+} cells purified by magnetic-activated cell sorting and sorted from spleen and lymph nodes of *Blimp1*$^{Bio/Bio}$*Rosa26*$^{BirA/BirA}$ mice were stimulated as described above, followed by chromatin precipitation by magnetic streptavidin or immunoglobulin G beads (Dynal) as described[56]. Precipitated DNA was quantified by real-time PCR analysis on a MyiQ (Bio-Rad) as described[57].

Real-time PCR analysis. Total RNA was prepared with the RNeasy kit (Qiagen) from CD4^{+}CD25^{+}GFP^{+}, CD4^{+}CD25^{+}GFP^{-}, CD4^{+}CD25^{-}CD62L^{-} and CD4^{+}CD25^{-}CD62L^{+} T cells purified by flow cytometry. Then, cDNA was synthesized from total RNA with random hexamers and SuperScript III reverse transcriptase (Invitrogen). Real-time PCR was done with the QuantiTect SYBR Green PCR kit (Qiagen; primer sequences, **Supplementary Methods**). Real-time PCR analysis of *Irf4* was done with a Taqman Gene Expression Assay (Applied Biosystems) and real-time PCR analysis of *Blimp1* was done with the Quantitect Primer Assay (Qiagen). Analyses were done in triplicate and mean normalized expression was calculated with the Q-Gene application with *Hprt1* as the reference gene[33].

***In vitro* suppression assays.** Suppression assays were done as described[26]. CD4^{+}CD25^{-} cells (responders) sorted by flow cytometry were used at a density of 2×10^4 cells per well and were cultured together with 8×10^4 irradiated splenocytes and a 1:2 'titration' of either GFP^{+} or GFP^{-} CD4^{+}CD25^{+} T cells as suppressors at a starting density of 8×10^4 cells per well in the presence of monoclonal anti-CD3 (0.5 μg/ml). Cells were cultured for 72 h and were pulsed with [^{3}H]thymidine (1 μCi per well) for the final 8 h of culture. Cells were collected and incorporation of [^{3}H]thymidine was measured by counting of scintillation with a MicroBeta TriLux 1450 Liquid Scintillation & Luminescence Counter (PerkinElmer).

Colitis model. Colitis was induced in *Rag1*$^{-/-}$ Ly5.1^{+} mice by intraperitoneal injection of 3.5×10^5 flow cytometry–sorted naive CD4^{+}CD25^{-}CD62L^{+} responder cells isolated from pooled spleens and lymph nodes of Ly5.1^{+} mice with or without 4×10^4 to 7.5×10^4 sorted GFP^{+} or GFP^{-} CD4^{+}CD25^{+} cells isolated from pooled spleens and lymph nodes of *Blimp1*$^{+/GFP}$ mice. Mice were monitored weekly for weight loss and were analyzed 8 weeks after cell transfer or when they had lost more than 10% of their body weight.

Retroviral transduction of T_{reg} cells and *Irf4*$^{-/-}$ T_{reg} cell 'rescue' experiments. Retroviral constructs were generated by cloning of full-length mouse *Irf4* or *Blimp1* cDNA into the pMIG retroviral vector. Retroviral supernatants

doi:10.1038/ni.2006

were generated by transient transfection of human embryonic kidney 293T cells with plasmids by calcium phosphate precipitation (CalPhos Mammalian Transfection kit; Clontech). Retrovirus was spun for 60 min at 2,500*g* and 4 °C onto plates coated with RetroNectin (Takara). T_{reg} cells purified by magnetic-activated cell sorting were cultured on plates coated with anti-CD3 in the presence of 100 U IL-2, 5 ng/ml of transforming growth factor-β (R&D Systems) and 2 μg/ml of anti-CD28. After 48 h, T_{reg} cells were cultured on retrovirus-coated plates in the presence of 2 μg/ml of polybrene and IL-2 for 1 more day before transfer into recipient mice. For the generation of recipient mice, fetal liver cells of *Foxp3*$^{-/-}$ embryos isolated at embryonic day 14.5 were used for reconstitution of hematopoiesis in lethally irradiated *Rag1*$^{-/-}$ mice. At 2 weeks after reconstitution, recipients were left untreated or were injected with T_{reg} cells purified from wild-type or *Irf4*$^{-/-}$ mice transduced with retroviral vector containing a GFP expression cassette only or GFP plus *Irf4* or *Blimp1* cDNA as described above. Recipient mice were analyzed 4 weeks after reconstitution.

IL-2–anti IL-2 experiments and T_H1 inflammation model. IL-2–anti-IL-2 complexes were produced by incubation (30 min at 37 °C) of 1.5 μg recombinant mouse IL-2 (eBioscience) with 7.5 μg monoclonal antibody to mouse IL-2 (JES6.1; produced 'in house') as described[35]. *Blimp1*$^{+/GFP}$ mice were injected intraperitoneally on days 0, 1 and 2 with either IL-2–anti-IL-2 complexes or PBS as a control and were collected on day 7. For analysis of T_{reg} cell differentiation under T_H1 inflammatory conditions, CD3ε-deficient mice were injected intravenously with 5×10^5 CD4$^+$CD25$^+$ cells enriched from pooled spleens and lymph nodes. Then, mice were injected intraperitoneally with 20 μg anti-CD40 (IC10; produced 'in house') on days 0, 2 and 4 after cell transfer. Donor cells were examined on day 6 (ref. 21).

Viral infections. Mice were inoculated intranasally with $1 \times 10^{4.5}$ plaque-forming units of the influenza virus strain HKx31 (H3N2) as described[58].

Statistics. Non-microarray data were analyzed with a two tailed, unpaired Student's *t*-test. *P* values of less than 0.05 were considered significant.

Microarray and binding sequence analysis. RNA was extracted from Blimp-1–GFP$^+$ T_{reg} cells from *Blimp1*$^{+/GFP}$ and *Blimp1*$^{GFP/GFP}$ mice. Three biological replicates of each were hybridized to Illumina mouse WG-6 Version 1.1 BeadChips at the Australian Genome Research Facility. Intensity values were background corrected and normalized by the neqc method[59]. Probes were filtered as 'not expressed' if they failed to achieve a BeadStudio detection *P* value of 0.1 on at least three arrays. Manufacturer probe annotation was used. Data from two replicates of RNA from *Irf4*$^{fl/+}$*Foxp3*-Cre and *Irf4*$^{fl/-}$*Foxp3*-Cre mice, hybridized to Affymetrix Mouse Genome 430 Version 2 Arrays, were obtained from a published study[18]. Affymetrix data were corrected for background and were normalized with the gcRMA algorithm. Probe sets were filtered as 'not expressed' if they failed to achieve a MAS5 'present call' on at least two arrays. Bioconductor probe set annotation was used. Differences in expression were assessed with empirical Bayes moderated *t*-statistics[60]. Genes were considered to have different expression if they achieved a false-discovery rate of less than 0.05 for the Blimp-1 data or unadjusted *P* value of less than 0.05 for the *Irf4* data. All analyses were done with Bioconductor software[61]. Probes were matched between platforms by Entrez Gene accession codes. Where there were multiple probes or probe sets for the same accession code, the probe with highest average expression was chosen. Overlap of gene lists in the *Blimp1*- and *Irf4*-based arrays was judged by Fisher's exact test. For further analysis and to account for intergene correlations, ROAST gene set tests[62] showed that a significant group of the Blimp-1 target genes were downregulated in IRF4-deficient cells ($P = 0.006$). The $\log_2$ 'fold' changes for *Rorc* and *Bcl2* in the *Irf4* data were averaged over multiple probe sets for these genes, and *P* values were combined *P* values from the ROAST gene set tests (**Supplementary Fig. 7b**). Searches for putative Blimp-1- and IRF4-binding sites in the *Il10* locus were made with the MATCH program in the TRANSFAC database[63]. The ClustalX program was used to align the sequence of first intron of mouse *Il10* to that of human *IL10* (ref. 64).

49. Malissen, M. *et al.* Altered T cell development in mice with a targeted mutation of the CD3-epsilon gene. *EMBO J.* **14**, 4641–4653 (1995).
50. Bouillet, P. *et al.* Proapoptotic Bcl-2 relative Bim required for certain apoptotic responses, leukocyte homeostasis, and to preclude autoimmunity. *Science* **286**, 1735–1738 (1999).
51. Szabo, S.J. *et al.* Distinct effects of T-bet in TH1 lineage commitment and IFN-γ production in CD4 and CD8 T cells. *Science* **295**, 338–342 (2002).
52. Kallies, A. *et al.* Initiation of plasma-cell differentiation is independent of the transcription factor Blimp-1. *Immunity* **26**, 555–566 (2007).
53. de Boer, E. *et al.* Efficient biotinylation and single-step purification of tagged transcription factors in mammalian cells and transgenic mice. *Proc. Natl. Acad. Sci. USA* **100**, 7480–7485 (2003).
54. Driegen, S. *et al.* A generic tool for biotinylation of tagged proteins in transgenic mice. *Transgenic Res.* **14**, 477–482 (2005).
55. Boyer, L.A. *et al.* Polycomb complexes repress developmental regulators in murine embryonic stem cells. *Nature* **441**, 349–353 (2006).
56. Ebert, A. *et al.* Novel regulatory elements with Pax5-dependent activity in pro-B cells are interspersed in the distal V_H gene cluster of the *Igh* locus. *Immunity* (in the press).
57. Decker, T. *et al.* Stepwise activation of enhancer and promoter regions of the B cell commitment gene *Pax5* in early lymphopoiesis. *Immunity* **30**, 508–520 (2009).
58. Flynn, K.J. *et al.* Virus-specific CD8$^+$ T cells in primary and secondary influenza pneumonia. *Immunity* **8**, 683–691 (1998).
59. Shi, W., Oshlack, A. & Smyth, G.K. Optimizing the noise versus bias trade-off for Illumina Whole Genome Expression BeadChips. *Nucleic Acids Res.* (in the press).
60. Smyth, G.K. Linear models and empirical Bayes methods for assessing differential expression in microarray experiments. *Stat. Appl. Genet. Mol. Biol.* **3**, article 3 (2004).
61. Gentleman, R.C. *et al.* Bioconductor: open software development for computational biology and bioinformatics. *Genome Biol.* **5**, R80 (2004).
62. Wu, D. *et al.* ROAST: rotation gene set tests for complex microarray experiments. *Bioinformatics* **26**, 2176–2182 (2010).
63. Kel, A.E. *et al.* MATCH: A tool for searching transcription factor binding sites in DNA sequences. *Nucleic Acids Res.* **31**, 3576–3579 (2003).
64. Jeanmougin, F. *et al.* Multiple sequence alignment with Clustal X. *Trends Biochem. Sci.* **23**, 403–405 (1998).